Calculation of linear and second-order optical response in wurtzite GaN and AlN

James L. P. Hughes, Y. Wang, and J. E. Sipe
Department of Physics, University of Toronto, Toronto, Ontario, Canada M5S 1A7
(Received 6 December 1996; revised manuscript received 3 February 1997)

We calculate the linear and nonlinear optical response of GaN and AlN in the wurtzite structure. The dielectric function $\epsilon(\omega)$, the second harmonic generation susceptibility $\chi^{(2)}(-2\omega;\omega,\omega)$, and the linear electro-optic susceptibility $\chi^{(2)}(-\omega;\omega,0)$ are all evaluated over a broad frequency range. These results are based on a first principles electronic structure calculation using the full-potential linearized augmented plane-wave method within the local density approximation. Corrections to the underestimation of the band gaps are included at the level of the scissors approximation, which is carefully incorporated within our susceptibility formalism. All independent components for the response functions are calculated; the results for GaN and AlN are very different, and those of AlN are in strong disagreement with predictions of the bond charge model. Results for all response functions at zero frequency are underestimated with respect to the available experimental values. A comparison of the calculated response functions for nonzero frequencies is made with the limited experimental data. We confirm both analytically and numerically that the calculated second-order susceptibilities obey various symmetry constraints below the band gap. [S0163-1829(97)04019-8]

I. INTRODUCTION

GaN and AlN are considered promising materials for various technological applications. The wide band gaps for these materials makes them candidates for use in the near-ultraviolet and ultraviolet regions. It has been suggested that GaN and AlN could be employed in nonlinear waveguides, short wavelength electroluminescent devices, and in high temperature diodes and transistors;[1–4] AlN has also been suggested as a frequency doubler for $Ga_xAl_{1-x}As$ laser diodes.[5,6] The high thermal conductivity and low compressibility of these materials are attractive mechanical properties for a range of device applications.[7]

There have been several experimental studies of the electronic and structural properties of these materials, as well as a number of investigations of the linear and nonlinear optical response.[1,4–6,8–11] Theoretical efforts, however, have been primarily concerned with ground state properties.[2,12–16] While there has been some work on linear optical response,[3,17,18] the only full band structure calculation of nonlinear response has been restricted to zero frequency.[19] In this context, it would be useful to have a comprehensive analysis of the optical properties of GaN and AlN, as determined from first principles, over a broad range of frequencies.

We have recently presented results on the linear and nonlinear optical properties of zinc-blende GaAs and GaP.[20] The goal of this work is to apply the analytic expressions and computational method employed there to the wurtzite materials GaN and AlN. Our evaluation of optical response is based on a first principles calculation of the electronic structure using the full-potential linearized augmented plane-wave (FLAPW) method.[21,22] We address the underestimation of the band gap by including self-energy corrections at the level of the scissors approximation.[20,23] This correction rigidly shifts the conduction states upward in energy and produces a corresponding change in the velocity matrix elements; the scissors correction is incorporated in a simple and straightforward way within our susceptibility formalism. The analytic expressions for the optical response functions are derived from the formalism of Sipe and Ghahramani[24] and Aversa and Sipe.[25] These expressions have the advantage of being inherently free of any unphysical divergences at zero frequency. Thus, we believe this constitutes a good initial approach to the *ab initio* determination of optical properties across a broad frequency range.

The calculational method and relevant susceptibility equations are briefly presented in Sec. II. In Sec. III we discuss and present the results of our first principles calculation. The band structures for these materials, as well as the linear and second-order optical response, are given in this section. We also identify the symmetries that the second-order response function satisfy, both analytically and numerically. Finally, in Sec. IV we present our conclusions.

II. CALCULATIONAL METHOD

In a previous paper[20] we detailed our method for calculating optical response in semiconductors. There we discussed the susceptibility notation and definitions, scissors approximation, electronic structure method, and the techniques employed in the Brillouin zone (BZ) integrations necessary for calculating the response functions. In the present work, our emphasis is on the results for the optical properties of GaN and AlN; we use the notation and definitions established in earlier work.[20] We seek the optical response above and below the band gap for these materials. For linear response, we evaluate the imaginary part of the dielectric function, $\epsilon_2(\omega)$, and then employ the Kramers-Kronig relations to obtain the real part of this function. Similarly, we have chosen to evaluate the imaginary part of the second harmonic generation (SHG) susceptibility, $\mathrm{Im}\{\chi^{abc}(-2\omega;\omega,\omega)\}$, and again obtain the real part using the Kramers-Kronig relations. This allows for the determination of the absolute value of this susceptibility over an energy spectrum above and below the band gap. We restrict our evaluation of the linear

electro-optic (LEO) susceptibility to the region strictly below the band gap. As this function is purely real in this region, we calculate it directly. The LEO susceptibility we consider here is in the clamped-lattice approximation.

In the calculation of the susceptibilities it is convenient to reduce the integration over the BZ to one over the irreducible segment of the BZ (IBZ). This is accomplished by applying the operators P_R of the group elements R of the hexagonal symmetry group $6mm$, appropriate for GaN and AlN, to the expansion dyadics of the response tensor. In the case of linear response, the dielectric tensor is given by

$$\vec{\vec{\epsilon}}(\omega)=\sum_{ab}\hat{a}\hat{b}\epsilon^{ab}(\omega), \tag{1}$$

and after applying the operators P_R we obtain

$$\sum_R P_R(\hat{x}\hat{x})=\sum_R P_R(\hat{y}\hat{y})=6\vec{\vec{1}},$$

$$\sum_R P_R(\hat{z}\hat{z})=12\vec{\vec{1}},$$

$$\sum_R P_R(\hat{a}\hat{b})=0, \quad a\neq b, \tag{2}$$

where $\vec{\vec{1}}$ is the identity tensor. Thus only the diagonal elements survive; contrary to what one obtains for materials with the cubic structure, all of these components are not equal. We can identify two independent components for the linear susceptibility, $\epsilon^{xx}=\epsilon^{yy}$, and ϵ^{zz}.

For second-order optical response we proceed in the same way. We can write the LEO susceptibility as

$$\vec{\chi}(-\omega;\omega,0)=\sum_{abc}\hat{a}\hat{b}\hat{c}\chi^{abc}(-\omega;\omega,0), \tag{3}$$

and applying the operators P_R we find

$$\sum_R P_R(\hat{z}\hat{z}\hat{z})=12(\hat{z}\hat{z}\hat{z}),$$

$$\sum_R P_R(\hat{x}\hat{x}\hat{z})=6(\hat{x}\hat{x}\hat{z}+\hat{y}\hat{y}\hat{z}),$$

$$\sum_R P_R(\hat{x}\hat{z}\hat{x})=6(\hat{x}\hat{z}\hat{x}+\hat{y}\hat{z}\hat{y}),$$

$$\sum_R P_R(\hat{z}\hat{x}\hat{x})=6(\hat{z}\hat{x}\hat{x}+\hat{z}\hat{y}\hat{y}),$$

$$\sum_R P_R(\hat{a}\hat{b}\hat{c})=0, \quad \text{all other } a,b,c. \tag{4}$$

We can identify four independent components for this second-order tensor, which we take to be χ^{zzz}, χ^{xxz}, χ^{xzx}, and χ^{zxx}. The same result follows for the SHG susceptibility with one exception: The SHG tensor possesses intrinsic permutation symmetry, or a symmetry in the permutation of the last two indices. This reduces the number of independent components to three, which for this tensor we take to be χ^{zzz}, χ^{xzx}, and χ^{zxx}.

To calculate the optical response functions it is necessary to perform an integration over the IBZ. Our approach towards this integration is to use a hybrid sampling-tetrahedron method. The essence of this method is to partition the IBZ into a large number of tetrahedra, at the vertices of which we calculate the eigenvalues and velocity matrix elements using the FLAPW method. We then sample a large number of points within each of these tetrahedra, linearizing quantities that appear in the integrand based on this vertex information. This approach is computationally efficient and provides an accurate integration over the entire IBZ; consequently, accuracy is maintained for energies above and below the band gap.

For the calculation of GaN and AlN we have partitioned the IBZ into 5184 tetrahedra, requiring a determination of the eigenvalues and velocity matrix elements at 1365 **k** points. In the case of GaN, we have further partitioned the region immediately near the Γ point into 3993 tetrahedra. This demands a further calculation of the eigenvalues and velocity matrix elements at an additional 1092 **k** points in this region. This is done for GaN only, as we present results on the anisotropy of the linear optical response function in the proximity of the band edge. To be confident in the accuracy of the calculation in this narrow energy region, the finer mesh of **k** points near the Γ point is required.

III. RESULTS AND DISCUSSION

A. Band structures

In Fig. 1 we present the band structures for GaN and AlN. In both cases the band gaps have been adjusted, via the scissors shift, to coincide with the experimental values. These band structures are in good agreement with other theoretical results based on various electronic structure methods within the local density approximation (LDA).[2,3,14,17] Agreement is somewhat less striking in a comparison of the eigenvalues at symmetry points from our band structure with existing quasiparticle calculations;[2] differences tend to be smaller than 0.4 eV for bands in proximity to the gap, and larger for bands further from the gap. We note that for these calculations, and all those discussed below, we have used the experimental values for the lattice constants;[26] for the crystal coordinate system, we have used the convention of Kobayashi and co-workers.[13]

In the all-electron calculation employed in this work, the $3d$ states in Ga have been explicitly included as valence states. These states encroach on the lowest valence states, as can be seen in the band structure between -10 and -15 eV. The inclusion of these states as part of the fully relaxed valence states in the calculation effects the appearance of these states in the band structure itself, and also affects the shape and position of the upper valence and lower conduction states. On this basis, we believe it is important to include these states in a full band structure calculation of the optical properties of GaN.

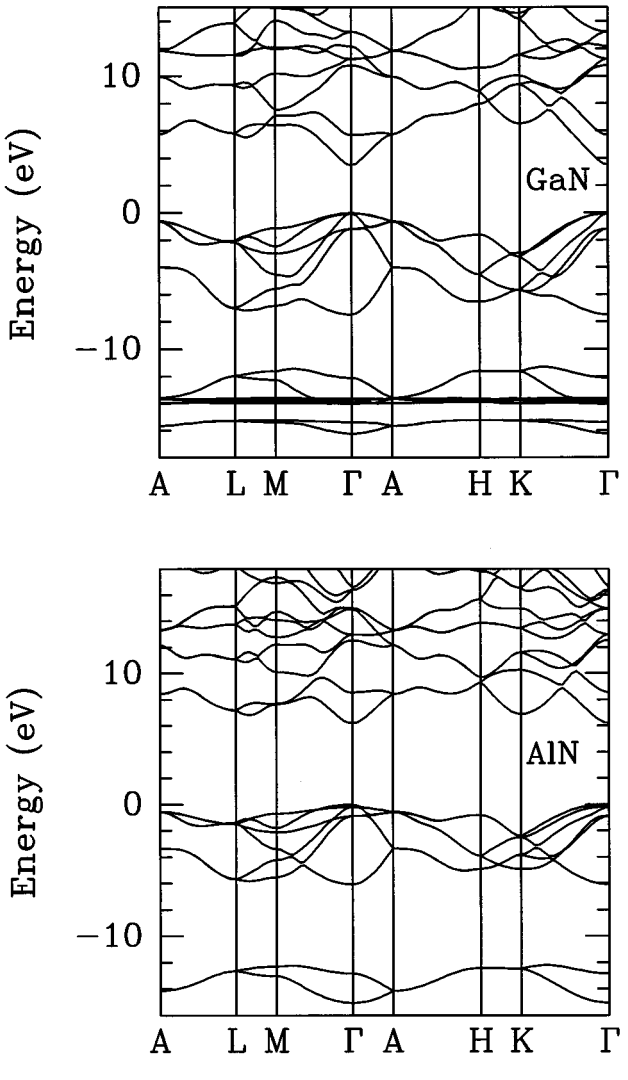

FIG. 1. FLAPW band structures for GaN (upper plot) and AlN (lower plot). The fundamental band gaps have been adjusted to 3.5 and 6.3 eV, respectively, within the scissors approximation.

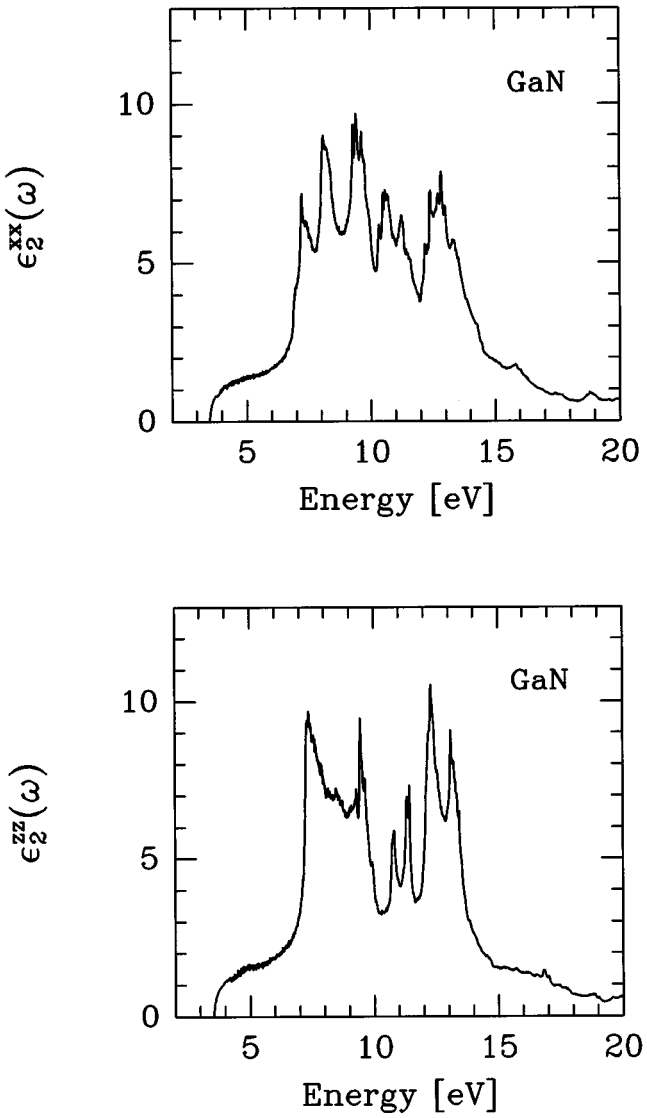

FIG. 2. Plot of the imaginary part of the dielectric function for GaN. Both independent components are plotted: $\epsilon_2^{xx}(\omega)$ (upper plot) and $\epsilon_2^{zz}(\omega)$ (lower plot).

B. Linear optical response

The results for linear optical response are presented in Fig. 2 and Fig. 3, again for GaN and AlN. In both figures we give our results for the two independent components of the imaginary part of the dielectric function, $\epsilon_2^{xx}(\omega)$ and $\epsilon_2^{zz}(\omega)$. The corresponding components of the two materials exhibit a general similarity, although the relative magnitudes of the peaks in the spectra of GaN differ significantly from those of AlN.

The general similarity of the $\epsilon_2(\omega)$ of these materials reflects the underlying similarity in the shapes of their band structures; the structural features in the $\epsilon_2(\omega)$ spectra are associated with regions in the band structure for which pairs of bands are nearly parallel and the joint density of states is high. In the column IV semiconductors and the III-V cubic semiconductors, it is usually possible to identify each peak with a parallel joint density of states in a specific band structure region. In contrast, for GaN and AlN we have only managed to construct a preliminary assignment of the different peaks. Similar efforts have previously been presented by other researchers.[3,27]

We begin with GaN. The first peak in both ϵ_2^{xx} (at 7.2 eV) and ϵ_2^{zz} (at 7.3 eV) is clearly due to the region between Γ and M in the Brillouin zone. The next two peaks in ϵ_2^{xx}, one at 8.1 eV and one at 9.5 eV, arise, respectively, from contributions from A to L and L to M, and from contributions from Γ to M and from A to H. In the place of these two peaks there is only one in ϵ_2^{zz} (at 9.5 eV), and it seems to arise from different regions in the Brillouin zone: Its main contributions come from the regions from H to K and from K to Γ. The next peak in each component (at 10.6 eV for ϵ_2^{xx} and at 10.8 eV for ϵ_2^{zz}) arises from contributions from Γ to A, from A to H, and from A to L; although obviously not well localized in the Brillouin zone, at least here there appears to be common sources for the strength in ϵ_2^{xx} and ϵ_2^{zz}. The sources of the remaining higher energy peaks are difficult to identify.

In AlN, where there are more peaks in each spectrum than in GaN, the identification of their origins is less clear. Here even the first peaks in the two components — at 8.7 eV in

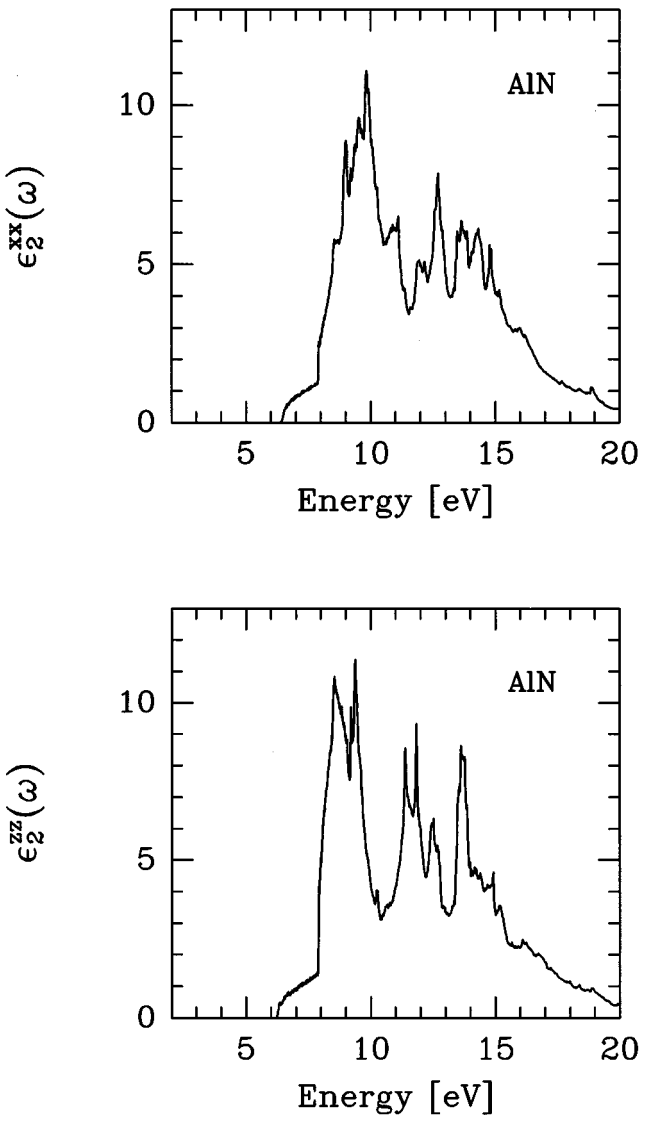

FIG. 3. Plot of the imaginary part of the dielectric function for AlN. Both independent components are plotted: $\epsilon_2^{xx}(\omega)$ (upper plot) and $\epsilon_2^{zz}(\omega)$ (lower plot).

ϵ_2^{xx} and at 8.5 eV in ϵ_2^{zz} — appear to have somewhat different origins. While the lowest energy peak in ϵ_2^{zz} arises from both the region from Γ to M that leads to the first peaks in the GaN spectra, and the region L to M, the lowest energy peak in ϵ_2^{xx} gains strength as well from the regions from Γ to A and A to L. The next four peaks in ϵ_2^{xx} (at 9.0 eV, coming from Γ to K; at 9.6 eV, coming from Γ to A, from A to H, and from L to A; at 9.8 eV coming from Γ to M; at 11.2 eV, the source of which we cannot identify) have only one counterpart in ϵ_2^{zz}, at 9.3 eV, with origins in the regions from Γ to K, from H to K, and from Γ to M. The two components both display a peak at 12.2 eV; in ϵ_2^{zz} this has its origins in the regions from Γ to A and from A to H, while in ϵ_2^{xx} there is as well a contribution from the region from L to H. We have not been able to identify well-defined regions in the Brillouin zone responsible for the other peaks.

Compared to the column IV elemental semiconductors and the III-V cubic semiconductors, the structure in $\epsilon_2(\omega)$ in GaN and AlN is considerably more complicated. This appears to arise in the large part because of the lower symmetry of the wurtzite structure, leading to a more complicated joint density of states than in the cubic materials and a resulting difficulty in assigning peaks to different regions in the Brillouin zone. Support for this comes from our calculation of the II-VI compound semiconductors, many of which can occur in both cubic and wurtzite form. Comparing $\epsilon_2(\omega)$ for the two structural forms of the same compound, we consistently find a more complicated spectrum for the wurtzite structure.[28]

Despite the complicated spectrum of $\epsilon_2(\omega)$ for GaN and AlN, our results are in good agreement with those of Christensen and Gorczyca[3] throughout the energy spectrum. Their calculation was based on the linear muffin-tin orbital (LMTO) method within the atomic-sphere approximation (ASA). Although, as they point out, their results are sensitive to the use of the ASA, we found a strong similarity between our results and theirs in the structure of the linear response function as well as in its value at zero frequency. These later results will be subsequently discussed. Solanki *et al.*[18] have also calculated the dielectric function for AlN using the LMTO-ASA method. These results show marked differences from our own. Their work illustrates the sensitivity of the linear response function to the application of the LMTO-ASA approach as well as the number of **k** points used in the calculation. Our results differ substantially both qualitatively and quantitatively from those of Xu and Ching:[17] Our structure of $\epsilon_2(\omega)$ for both GaN and AlN is in disagreement with theirs in respect to both peak positions and relative peak magnitudes. In addition, they found anomalously large values for $\epsilon_2(\omega)$ for GaN for energies in excess of 20 eV. We found no such increase in the linear response in this region.

The only experimental data for $\epsilon_2(\omega)$ of which we are aware is the spectroscopic ellipsometry measurements for GaN of Petalas *et al.*[4] This data does not exhibit the degree of structure that is present in our calculation, but does show general agreement in peak positions.

As there is interest in near band edge optical response, we present in Fig. 4 the GaN results for $\epsilon_2(\omega)$ in the region near the function onset. Both independent components are plotted so as to elucidate the anisotropy of the function in this region. Our calculation indicates a difference in $\epsilon_2(\omega)$ for the two components of about 0.02 for energies within 0.05 eV of the band gap, increasing to a maximum difference of 0.2 up to about 7 eV; the magnitude of the difference varies quite strongly with energy throughout this range. It should be noted that our calculation does not take into account excitonic effects which are known to affect the shape of the linear response function near the band edge.

C. Second-order optical response

We present our results for the imaginary part of the SHG susceptibility in Fig. 5 for GaN and AlN. We have plotted the three independent components of this function for each material. A striking feature of the results, particularly in comparison with those for the zinc-blende semiconductors,[20] is how structured the frequency dependence is for all components of both materials. As in $\epsilon_2(\omega)$, this appears to be due in large part to the lower wurtzite symmetry of these

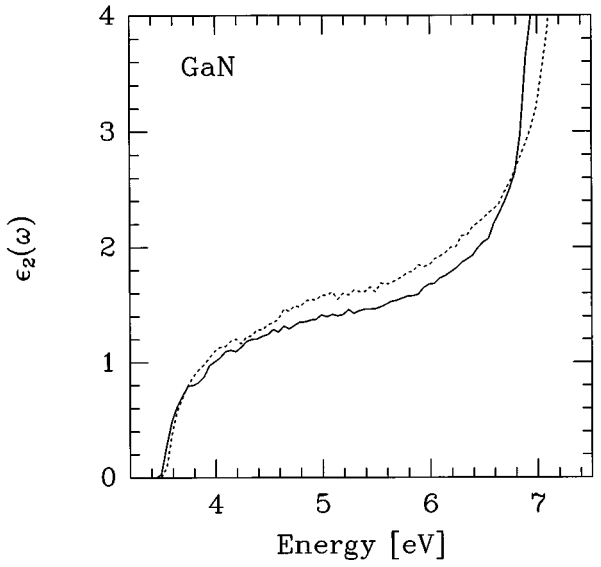

FIG. 4. Results for the calculated imaginary part of the dielectric function in the energy region near the function onset: $\epsilon_2^{xx}(\omega)$ (solid line) and $\epsilon_2^{zz}(\omega)$ (dotted line).

compounds. It is difficult to interpret the structure in $\chi^{(2)}$ in terms of the band structure of the material — especially for the wurtzite structure — because one must consider both one- and two-photon resonances in various regions of the band structure, and the interference between these processes. An initial attempt is made at this below; it is clear, however, that there is virtually no similarity between the results for these two compounds. Particularly considering the similarities in the linear optical response of these two materials, this highlights the greater sensitivity of the second-order response function to details of the band structure and momentum matrix elements of the material.

The imaginary part of the SHG susceptibility for GaN is initially very flat for all components in a region of approximately 1 eV near the half band gap. Beyond this region the structure of the response function, as well as the differences between individual components, becomes dramatically more pronounced. Our results show a strong similarity between the χ^{xzx} and χ^{zxx} components over the entire energy spectrum. To a large degree, peak position and magnitude is approximately the same for both components. The χ^{zzz} component exhibits a similar general structure, but is opposite in sign and larger in magnitude than the other two components. We will address this relationship between the magnitudes of the components in a subsequent discussion of the predictions of the bond charge approach.

The spectrum of the imaginary part of the SHG susceptibility for AlN bears little resemblance to that of GaN. There appears to be no definite relationship between the independent components for this function. However, in general, the χ^{zzz} component is usually the largest of the three components throughout the energy spectrum.

Turning now to the details of the peaks, for GaN we first consider the χ^{zzz} component. The broad peak between 3.7 and 4.6 eV seems to be attributable to a two photon resonance associated with the first peak in the ϵ_2^{xx} spectrum, but with an increasing contribution, at an increasing energy,

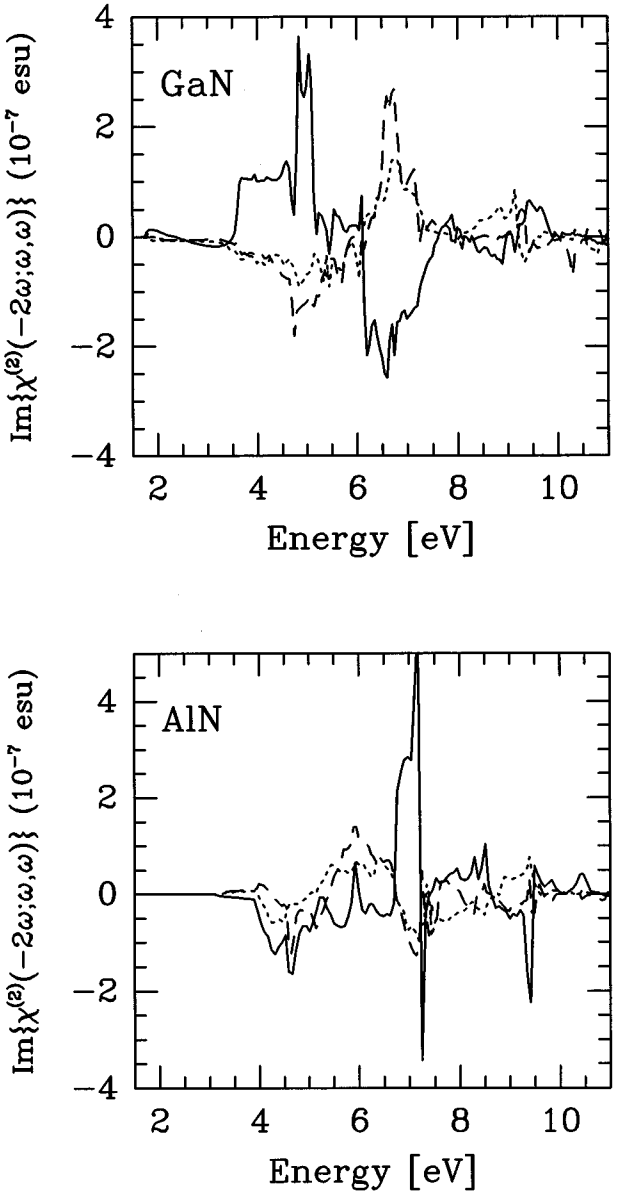

FIG. 5. Imaginary part of the SHG susceptibility $\mathrm{Im}\{\chi^{abc}(-2\omega;\omega,\omega)\}$ for GaN (upper plot) and AlN (lower plot). The three independent components are plotted: χ^{zzz} (solid line), χ^{xzx} (dotted line), and χ^{zxx} (dashed line). The energy bin size is 0.05 eV.

from a two photon resonance associated with the second peak in the ϵ_2^{zz} spectrum. The peaks at 6.2 and 6.7 eV are most likely due to two photon resonances associated with the fifth and sixth peaks in the ϵ_2^{zz} spectrum. For the χ^{zxx} component, the first main peak at 4.7 eV is due to a two photon resonance associated with the second peak in the ϵ_2^{zz} response function. The peak at 5.7 eV is most likely from two photon resonances associated with the fifth peak in ϵ_2^{xx} and the fourth peak in ϵ_2^{zz}. Finally, the small peak at 7.2 eV is attributable to one photon resonances associated with the first peaks in both ϵ_2^{xx} and ϵ_2^{zz}. The χ^{xzx} component is the most difficult to interpret in terms of the band structure. We can only loosely identify the peak at 4.8 eV with a two photon resonance associated with the third peak in ϵ_2^{xx}, and

the peak at 6.7 eV with a two photon resonance associated with the sixth peak in the ϵ_2^{zz}.

For AlN, the χ^{zzz} component has two peaks for which somewhat definitive statements can be made. The first is the peak at 4.3 eV, which is due to two photon resonances associated with the first peaks in both ϵ_2^{xx} and ϵ_2^{zz}. The peak at 5.9 eV is probably due to a two photon resonance associated with the fourth peak in ϵ_2^{zz}. We note, however, that we were unable to specify a band structure region contributing to this peak. For the χ^{zxx} component the peak at 4.7 eV is due to a two photon resonance associated with the second peak in ϵ_2^{zz}. The peak at 5.9 eV again seems associated with the fourth peak in ϵ_2^{zz}, as for the χ^{zzz} component. Again, the contributions to the χ^{xzx} component are very hard to determine. We can only suggest that the peak at 4.3 eV is from two photon transitions associated with the first peak in both ϵ_2^{xx} and ϵ_2^{zz}.

In Fig. 6 we plot the absolute value of the SHG susceptibility for both materials. Features of these results which merit noting are as follows: The χ^{zzz} component dominates in both spectra for virtually all energies. In GaN all three components are of comparable size for energies below the half band gap, whereas in AlN the χ^{xzx} and χ^{zxx} components are substantially smaller than the χ^{zzz} component. GaN exhibits significantly more structure for energies around the half band gap than does AlN.

The results presented in this paper are, to our knowledge, the first for the SHG susceptibility beyond zero frequency. There are, however, experimental results with which we can compare. Considerable work has been done by Miragliotta *et al.* on the nonlinear optical response of GaN. Results for $\chi^{zxx}(-2\omega;\omega,\omega)$ have been presented for energies around the half band gap.[11] We have plotted in Fig. 7 these experimental results along with our calculated results for the absolute value of $\chi^{zxx}(-2\omega;\omega,\omega)$. This data roughly exhibits the same structure as our theoretical calculation in that this function decreases towards the half band gap and then increases from there for higher energies. But the magnitude of the experimental data is approximately twice that of our calculated values. For AlN the experimental data is somewhat less complete. Over a range of energies, the only data of which we are aware is that of Lundquist *et al.*[5,6] on radio-frequency sputter deposited AlN thin films. The experimental results exhibit a remarkably similar dispersion to our theoretical predictions, but are about 40% smaller in magnitude. It has been suggested by this experimental group that the value of the measured SHG susceptibility can be expected to increase with improved crystallinity of the AlN film; it is not clear how much larger this response function might become.

The value of the SHG susceptibility at zero frequency was the focus of the only other full band structure work on the nonlinear optical properties of GaN and AlN.[19] For this reason, and the fact that some low frequency experimental data has been presented in the literature, it is important that we place our work within this context. In Table I we present our results for the dielectric function, and the SHG susceptibility at zero frequency for GaN and AlN. We have also included the values from other theoretical calculations and experiments. We have only included two components for the SHG response function, as the χ^{xzx} and χ^{zxx} components are identical in the limit that the frequency approaches zero.

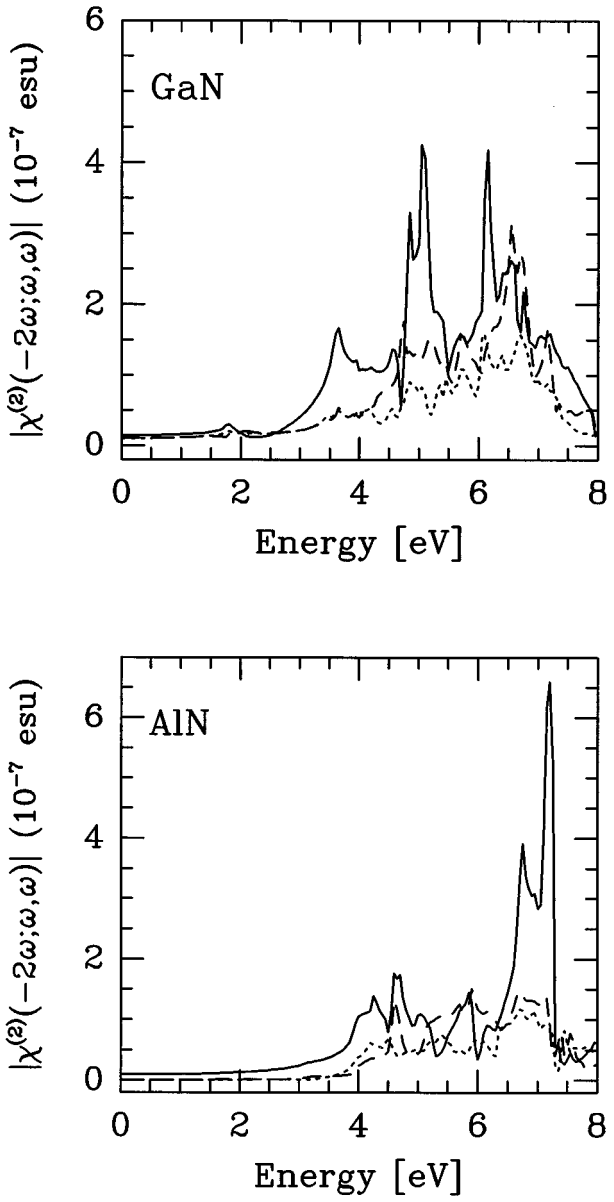

FIG. 6. Absolute value of the SHG susceptibility above and below the band gap for GaN (upper plot) and AlN (lower plot). The independent components are χ^{zzz} (solid line), χ^{xzx} (dotted line), and χ^{zxx} (dashed line).

The results of the current calculation for the linear optical response at zero frequency are very close to those of the LMTO-ASA work of Christensen and Gorczyca[3] as well as the pseudopotential calculation of Chen *et al.*[29] (where they have included the scissors approximation). There is some disagreement regarding the anisotropy of the dielectric function at zero frequency, although this anisotropy is not calculated to be large for either material. Our results as well as the other two calculations predict values for $\epsilon_2(0)$ smaller than the available experimental results. This result is striking in that our previous calculation for GaAs and GaP obtained values for the zero frequency linear response that were excellent in comparison with experiment. This may point to a

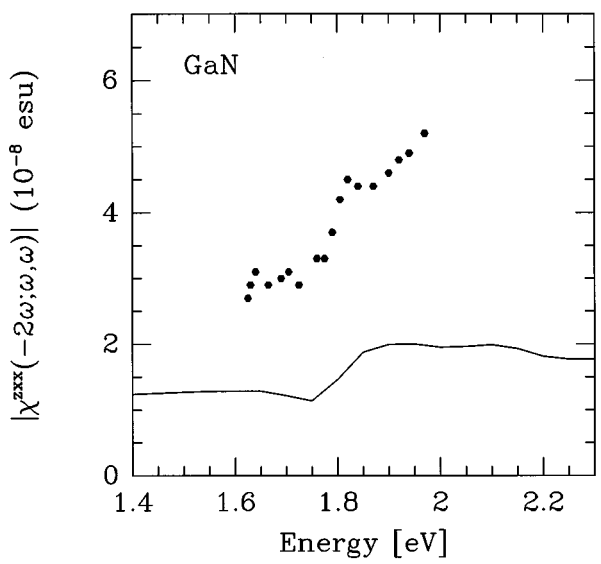

FIG. 7. The absolute value of $\chi^{zxx}(-2\omega;\omega,\omega)$ (solid line) plotted with the experimental data from Miragliotta *et al.* (Ref. 11) (solid circles).

limitation in the scissors approximation or, in the case of the LMTO method, to the use of ''corrective'' terms to adjust the LDA band gaps. It has been suggested that for wide band gap materials the scissors approach may be inadequate for correctly predicting zero frequency response.[30] The pseudopotential calculation of Chen *et al.*,[19] which does not employ the scissors correction, suffers from the usual LDA band gap problem in that the band gap is underestimated. This naturally leads to higher values for the dielectric function at zero frequency. The only wildly anomalous results are those of Xu and Ching[17] using the orthogonalized linear combination of atomic orbitals (OLCAO) method. Their values are exceedingly large for GaN, and predict a strong anisotropy. For AlN, the $\epsilon_2^{xx}(0)$ value is close to other calculations, but again a large anisotropy is predicted leading to a large value for $\epsilon_2^{zz}(0)$.

For the SHG susceptibility at zero frequency the theoretical and experimental data is more scarce. We find that our results are very close to those of Chen *et al.*[29] when they have incorporated the scissors correction. Again, their results without the scissors correction will be higher due to an underestimation of the band gap. The theoretical calculations predict values for the SHG susceptibility lower than those measured experimentally for both GaN and AlN. The experimental data for GaN is opposite in sign to the calculated values, but as Chen *et al.*[19] point out, the overall sign was not experimentally determined relative to the atomic coordinates.

One of the values of full band structure calculations such as ours is that they provide a check on simpler models for optical response that are often employed in the absence of more detailed calculations. For example, the usual bond charge model for $\chi^{(2)}$ (Ref. 31) predicts that the χ^{zzz} component should be twice as large as the χ^{xzx} component, but of opposite sign. It is based on the assumptions of perfect tetrahedral bonding and an optical response consisting of independent electrons moving only along the direction of their bonds. Our present work finds that the bond charge prediction for χ^{zzz}/χ^{xzx} holds only approximately for GaN; indeed, the bond charge prediction holds to a good approximation not only at zero frequency, where the bond charge model is usually applied, but as well for the ratio of the components of $\mathrm{Im}\{\chi^{(2)}(-2\omega;\omega,\omega)\}$ throughout a large energy range, as can be seen in Fig. 5. Yet the bond charge prediction fails completely for AlN. This result has already been found by Chen *et al.*,[19] and is thus independently confirmed here.

The simplest possible reason for the difference between the two materials is that the lattice structure of AlN implies a

TABLE I. The dielectric function and the SHG susceptibility at zero frequency. Results of the present calculation (FLAPW) are compared with other theoretical calculations and experimental data. The experimental data for SHG is extrapolated to zero frequency following Chen *et al.* (Ref. 19). The values for $\chi^{(2)}(0)$ are in pm/V.

Material	Method	$\epsilon^{xx}(0)$	$\epsilon^{zz}(0)$	$\chi^{zzz}(0)$	$\chi^{xzx}(0)$
GaN	FLAPW	4.82	4.80	6.03	-4.27
	Pseudopot. (no scissors; LDA gap)	5.54[a]	5.60[a]	10.8[b]	-6.4[b]
	Pseudopot. (scissors)[b]	4.75	4.85	7.0	-4.2
	LMTO-ASA[c]	4.71	4.62		
	OLCAO[d]	8.72	11.16		
	Experiment	5.2[e]		-10.7[f]	5.3[f]
AlN	FLAPW	3.91	3.97	-3.77	-0.25
	Pseudopot. (no scissors; LDA gap)	4.42[a]	4.70[a]	-8.4[b]	-0.2[b]
	Pseudopot. (scissors)[b]	3.78	3.94	-4.6	-0.2
	LMTO-ASA[c]	3.91	3.77		
	OLCAO[d]	3.88	5.06		
	Experiment	4.68[g]		-12.6 ± 7[h]	$\leqslant\lvert 0.5\rvert$[h]

[a]Reference 19.
[b]Reference 29.
[c]Reference 3.
[d]Reference 17.
[e]Reference 36.
[f]Reference 1.
[g]Reference 37.
[h]Reference 9.

bonding structure much further than that of GaN from the perfect tetrahedral bonding usually assumed. This, however, is clearly not the whole story: Relaxing *only* the assumption of perfect tetrahedral bonding and using the actual lattice parameters of GaN and AlN, the so-revised bond charge model would predict a χ^{zzz}/χ^{xzx} ratio of -2.053 for GaN, and a ratio of -2.208 for AlN. Clearly the correction for GaN is small and that for AlN is substantial; yet the disagreement of our results for AlN with even this revised bond charge model is poor. Obviously other assumptions of the bond charge model are in error. The results of Xu and Ching[17] for the ground state charge density contours indicated bonding of considerably more covalent character in GaN than in AlN; our results for density contours confirm this. While what is really of essence is the nature of the charge density response to applied fields, the nature of the ground states at least suggests that the model of directional bonds is, in general, more appropriate for GaN than AlN. This is clearly a qualitative issue worthy of more study.

We present our results for the clamped-lattice LEO coefficient in Fig. 8 for both materials. We have evaluated this function strictly below the band gap. To our knowledge these are the first *ab initio* calculations of the LEO susceptibility for these materials. We have plotted the four independent components of this response function, but note that for energies below the gap the χ^{xzx} and χ^{zxx} components are identical. This response function gradually increases in magnitude as the energy moves towards the band gap, where it experiences a resonance enhancement. For both materials the χ^{zzz} component is the largest. In GaN the other components are approximately half as large and opposite in sign. In the case of AlN the remaining components are very small in relation to the χ^{zzz} component. These results are not surprising given the data we have presented for the SHG susceptibility.

We are aware of only one experimental determination of the LEO coefficient for these materials. Long *et al.*[32] have measured this coefficient for GaN at 1.96 eV and obtained $\chi^{zzz}=30\pm5.5$ pm/V and $\chi^{xzx}=9\pm1.7$ pm/V. They have not determined the absolute sign of this response function. Our calculated results at this energy for comparison are $\chi^{zzz}=7$ pm/V and $\chi^{xzx}=6$ pm/V. This comparison is however not strict; we calculated the LEO susceptibility in the clamped-lattice approximation while the experimental data is for the total LEO effect.

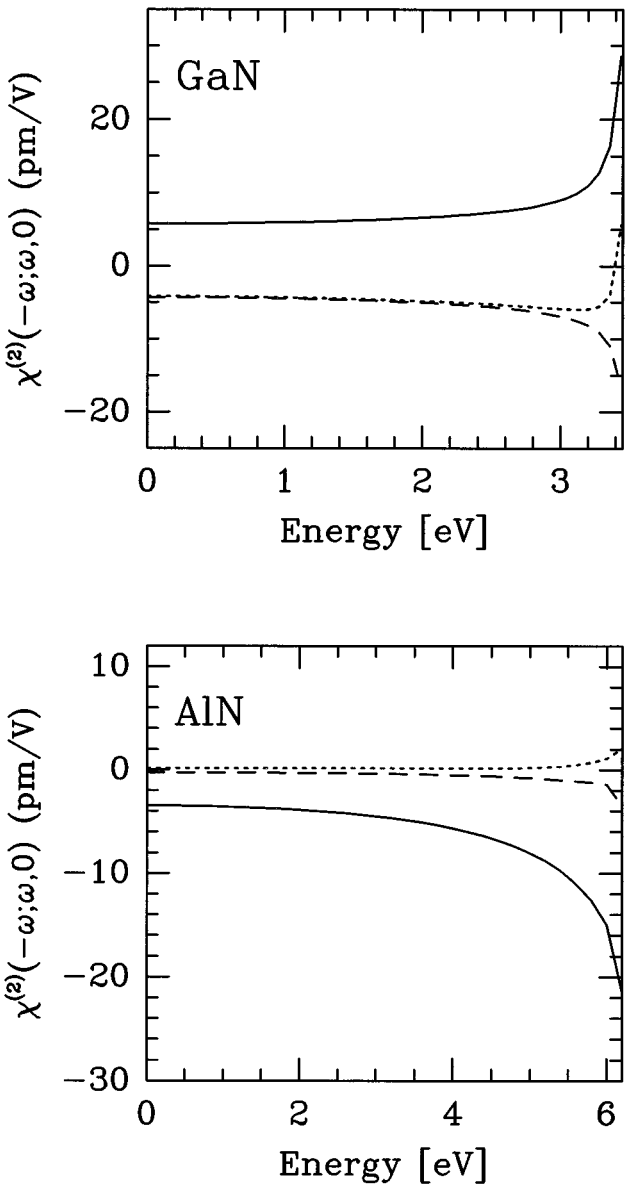

FIG. 8. Plot of the LEO susceptibility below the band gap for GaN (upper plot) and AlN (lower plot). The four independent components are plotted: χ^{zzz} (solid line), χ^{xzx} and χ^{zxx} (dotted line), and χ^{xxz} (dashed line). Note that two of the components are coincident in this energy region.

D. Symmetries of $\chi^{(2)}$

The nonlinear optical susceptibilities are required to satisfy certain symmetry considerations and constraints.[33] It is the goal of this section to state some of these conditions and demonstrate how our calculation satisfies them.

We first consider intrinsic permutation symmetry in the case of the SHG response function. As has been previously presented,[20] our susceptibility expression is written so as to explicitly satisfy this symmetry constraint. We have already discussed this in Sec. II regarding the reduction of the independent components for the SHG function from four to three, but for completeness mention it here.

For energies at which there is no absorption (below the band gap), full permutation symmetry holds. In terms of the LEO susceptibility this demands that

$$\chi^{zxx}(-\omega;\omega,0)=\chi^{xzx}(-\omega;\omega,0). \tag{5}$$

As indicated in Fig. 8 these two components have been numerically shown to be identical below the band gap. This symmetry condition can also be shown to hold true analytically within our susceptibility formalism.

We next consider Kleinman symmetry[34] which holds for very low frequencies. This symmetry could be written schematically as

$$\lim_{\omega\to0}\chi^{xxz}=\lim_{\omega\to0}\chi^{xzx}=\lim_{\omega\to0}\chi^{zxx}, \tag{6}$$

either for the LEO or SHG coefficient, and for them interchangeably. Again Fig. 8 illustrates how this symmetry has been numerically satisfied by our calculation; three of the

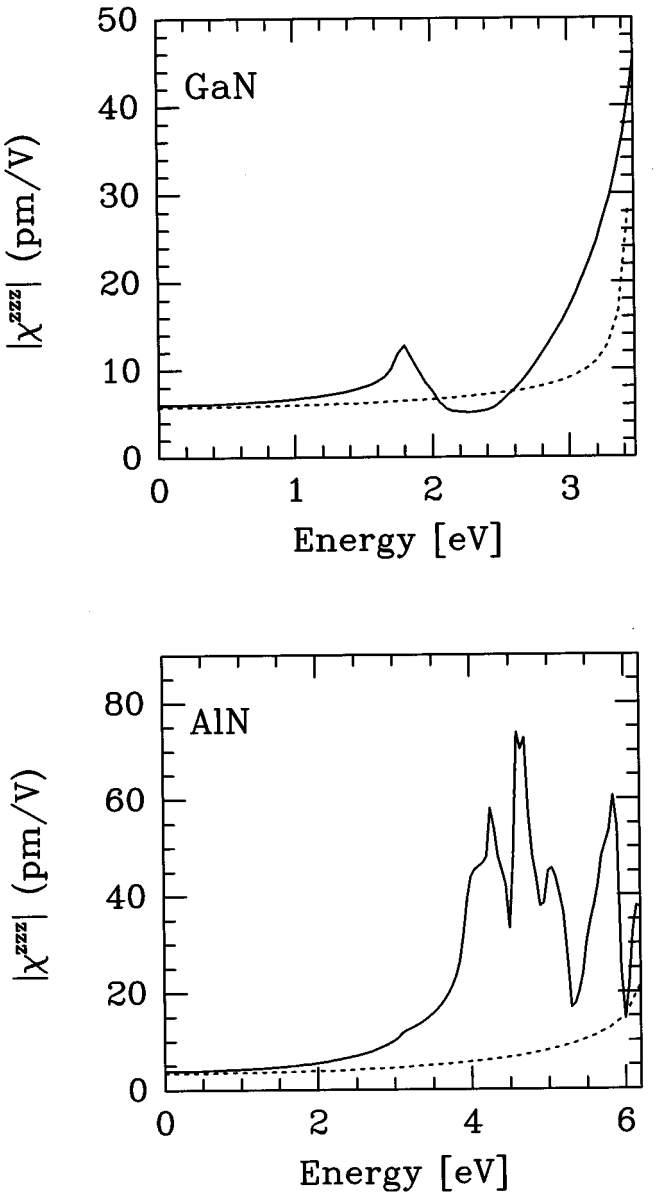

FIG. 9. Absolute value of the second-order optical response functions for GaN (upper plot) and AlN (lower plot) below the band gap. The χ^{zzz} component has been plotted for the SHG susceptibility (solid line), and the LEO susceptibility (dotted line).

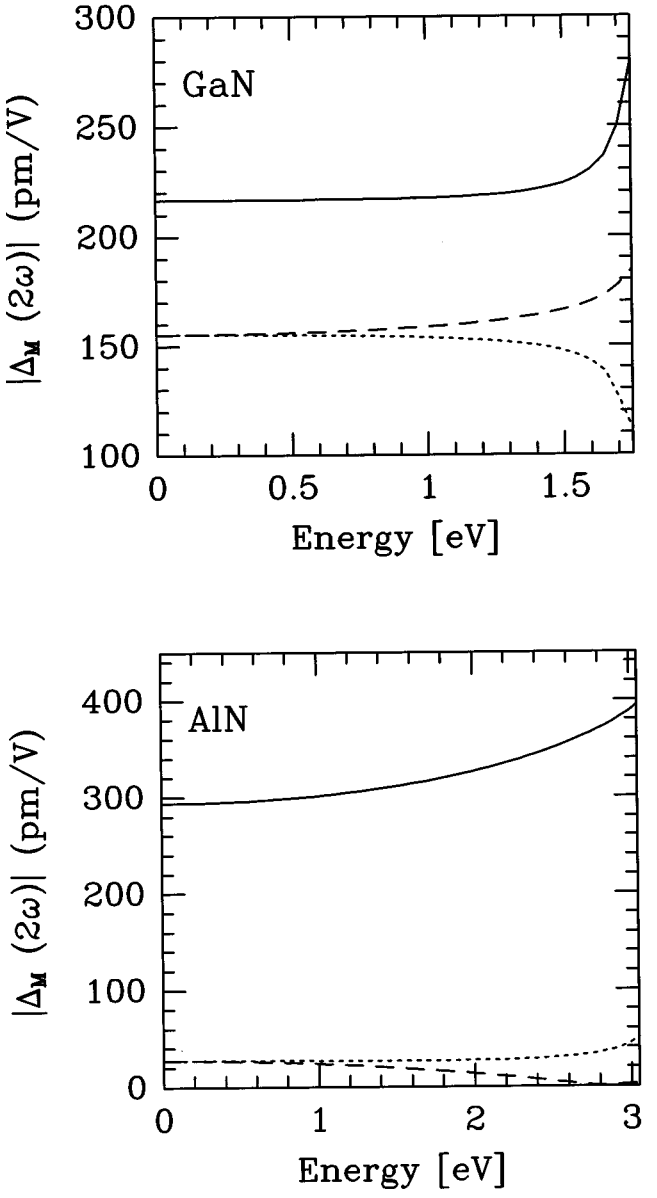

FIG. 10. Plot of Miller's $\Delta_M(2\omega)$ below the half band gap for GaN (upper plot) and AlN (lower plot). The three independent components are plotted: Δ^{zzz} (solid line), Δ^{xzx} (dotted line), and Δ^{zxx} (dashed line).

independent components for the LEO susceptibility are equal in the limit of zero frequency. This symmetry constraint can also be shown to hold in Fig. 6 for the SHG susceptibility. In this case two of the three independent components are numerically identical in the zero frequency limit; the expressions can also be shown to be equivalent analytically.

Finally, a condition that one would expect on physical grounds is that as the frequency approaches zero, the second-order response functions become equal. This can be written as

$$\lim_{\omega\to 0}\chi^{abc}(-2\omega;\omega,\omega)=\lim_{\omega\to 0}\chi^{abc}(-\omega;\omega,0). \qquad (7)$$

We have discussed and numerically demonstrated this condition in a previous paper in the case of GaAs and GaP. Here we can illustrate how this condition holds for GaN and AlN in the wurtzite structure by plotting the SHG and LEO susceptibilities on the same graph. In Fig. 9 we have plotted the χ^{zzz} component for each material. This figure clearly shows how both of these susceptibilities are equal for vanishing frequency; again, analytic equivalence can be demonstrated.

The above susceptibility constraints should hold in any calculational approach, and they provide a solid check of not only our formalism but of our numerical method.

E. Miller's δ

We have previously calculated Miller's δ for GaAs and GaP (Ref. 20) and there found reasonable support for some of Miller's original predictions about this function. It is useful, therefore, to calculate Miller's δ for the semiconductors in this work.

A generalized form of Miller's δ for SHG can be written as

$$\Delta_M^{abc}(2\omega)=\frac{\chi^{abc}(-2\omega;\omega,\omega)}{\chi^{aa}(2\omega)\chi^{bb}(\omega)\chi^{cc}(\omega)}. \tag{8}$$

We plot in Fig. 10 the three independent components of this function for GaN and AlN, respectively. Our results indicate that the assumption of frequency independence of this function largely holds over a broad frequency range. We note, however, that there are obvious deviations from Miller's assumption of material independence for the value of a given Δ_M function. The values for Δ_M^{zzz} differ by about 30% over much of the frequency range. The other independent components are very different for different materials. This later result we might expect given that the ratios of the magnitudes of independent components differ dramatically for GaN and AlN as has already been discussed. For comparison we note that the zero frequency values of Δ_M^{xyz} that we previously obtained for GaAs and GaP are 194 and 198 pm/V,[20] respectively. Levine[35] has also calculated Δ_M^{xyz} for GaAs and GaP and has obtained 347 and 310 pm/V, respectively.

IV. CONCLUSIONS

We have presented results for the optical response of wurtzite GaN and AlN for a broad range of energies. This work has employed a first principles electronic structure calculation in the FLAPW method, and a completely nondivergent formalism for the optical susceptibilities. The scissors approximation has been incorporated in our calculation in an attempt to correct for the underestimated LDA band gaps.

Our results for linear optical response show striking similarities to those of Christensen and Gorczyca.[3] We are, however, in strong disagreement with other theoretical calculations. Our zero frequency results, in line with those of other workers, underestimate the experimental values. We predict a very small anisotropy at zero frequency as well as a relatively small anisotropy in $\epsilon_2(\omega)$ for GaN for energies within 3 eV of the band gap.

Our work on second-order optical response constitutes the first comprehensive calculation and analysis for GaN and AlN over a broad energy range. We have calculated all independent components for the SHG and LEO susceptibilities and our results indicate strong dissimilarities between the materials considered in this work. The calculated spectrum of the SHG susceptibility for both materials is extremely rich in structure with the general feature of a dominant χ^{zzz} component. For energies below the gap, the other independent components are very small by comparison in AlN, but are of comparable magnitude in GaN. The predictions of the bond charge method seem to hold only approximately in GaN and fail completely for AlN. This we can attribute, only in part, to the greater degree of tetrahedral bonding in GaN.

Our calculated values for the second-order susceptibilities are smaller than the available experimental data by approximately a factor of two. We note, however, that very little experimental data exists for a range of energies above and below the band gap, and for very low energies for which zero frequency results can be equated.

We have also detailed some of the symmetry properties that the second-order susceptibilities must satisfy. These constraints have been demonstrated to be adhered to numerically and are satisfied analytically within our susceptibility formalism.

ACKNOWLEDGMENTS

The authors wish to thank Professor Henry Krakauer of the College of William and Mary for providing us with the FLAPW program. We thank Dr. E. Ghahramani for discussions on this and our earlier calculations (Ref. 20). This work is supported by the Natural Sciences and Engineering Research Council of Canada and the Ontario Laser and Lightwave Research Centre.

[1] J. Miragliotta, D. K. Wickenden, T. J. Kistenmacher, and W. A. Bryden, J. Opt. Soc. Am. B **10**, 1447 (1993).
[2] A. Rubio *et al.*, Phys. Rev. B **48**, 11 810 (1993).
[3] N. E. Christensen and I. Gorczyca, Phys. Rev. B **50**, 4397 (1994).
[4] J. Petalas *et al.*, Phys. Rev. B **52**, 8082 (1995).
[5] W. P. Lin *et al.*, Appl. Phys. Lett. **63**, 2875 (1993).
[6] P. M. Lundquist *et al.*, Appl. Phys. Lett. **65**, 1085 (1994).
[7] S. Strite, M. E. Lin, and H. Morkoc, Thin Solid Films **213**, 197 (1993).
[8] P. Perlin *et al.*, Phys. Rev. B **45**, 13 307 (1992).
[9] Y. Fujii *et al.*, Appl. Phys. Lett. **31**, 815 (1977).
[10] J. Miragliotta and D. K. Wickenden, Phys. Rev. B **50**, 14 960 (1994).
[11] J. Miragliotta, W. A. Bryden, T. J. Kistenmacher, and D. K. Wickenden, in *Diamond, SiC and Nitride Wide Bandgap Semiconductors*, edited by C. H. Carter, Jr., G. Gildenblat, S. Nakamura, and R. J. Nemanich, MRS Symposia Proceedings No. 339 (Materials Research Society, Pittsburgh, 1994).
[12] W. Y. Ching and B. N. Harmon, Phys. Rev. B **34**, 5305 (1986).
[13] A. Kobayashi, O. F. Sankey, S. M. Volz, and J. D. Dow, Phys. Rev. B **28**, 935 (1983).
[14] M. Suzuki, T. Uenoyama, and A. Yanase, Phys. Rev. B **52**, 8132 (1995).
[15] E. Ruiz, S. Alvarez, and P. Alemany, Phys. Rev. B **49**, 7115 (1994).
[16] A. Rubio, J. L. Corkill, and M. L. Cohen, Phys. Rev. B **49**, 1952 (1994).
[17] Y.-N. Xu and W. Y. Ching, Phys. Rev. B **48**, 4335 (1993).
[18] A. K. Solanki *et al.*, Solid State Commun. **94**, 1009 (1995).
[19] J. Chen, Z. H. Levine, and J. W. Wilkins, Appl. Phys. Lett. **66**, 1129 (1995).
[20] J. L. P. Hughes and J. E. Sipe, Phys. Rev. B **53**, 10751 (1996).
[21] H. Krakauer, M. Posternak, and A. J. Freeman, Phys. Rev. B **19**, 1706 (1979).
[22] E. Wimmer, H. Krakauer, M. Weinert, and A. J. Freeman, Phys. Rev. B **24**, 864 (1981).
[23] Z. H. Levine and D. C. Allan, Phys. Rev. Lett. **63**, 1719 (1989).
[24] J. E. Sipe and E. Ghahramani, Phys. Rev. B **48**, 11 705 (1993).
[25] C. Aversa and J. E. Sipe, Phys. Rev. B **52**, 14 636 (1995).
[26] *Physics of Group IV Elements and III-V Compounds*, edited by

K. Hellwege, and O. Madelung, Landölt-Bornstein, New Series, Group III, Vol. 17, Pt. a (Springer, New York, 1982).
[27] M. L. Cohen and J. R. Chelikowsky, *Electronic Structure and Optical Properties of Semiconductors* (Springer-Verlag, New York, 1989).
[28] J. L. P. Hughes and J. E. Sipe (unpublished).
[29] J. Chen (private communication).
[30] J. Chen, Z. H. Levine, and J. W. Wilkins, Phys. Rev. B **50**, 11 514 (1994).
[31] B. F. Levine, Phys. Rev. B **7**, 2600 (1973).
[32] X. C. Long *et al.*, Appl. Phys. Lett. **67**, 1349 (1995).
[33] R. W. Boyd, *Nonlinear Optics* (Academic Press, San Diego, 1992).
[34] D. A. Kleinman, Phys. Rev. **126**, 1977 (1962).
[35] Z. H. Levine, Phys. Rev. B **49**, 4532 (1994).
[36] E. Ejder, Phys. Status Solidi A **5**, 445 (1971).
[37] L. Akasaki and M. Hashimoto, Solid State Commun. **5**, 851 (1967).